Journal of Biological Research

Bollettino della Società Italiana di Biologia Sperimentale



eISSN 2284-0230 - pISSN 1826-883

https://www.pagepressjournals.org/index.php/jbr/index

Publisher's Disclaimer. E-publishing ahead of print is increasingly important for the rapid dissemination of science. The ***Early Access*** service lets users access peer-reviewed articles well before print / regular issue publication, significantly reducing the time it takes for critical findings to reach the research community.

These articles are searchable and citable by their DOI (Digital Object Identifier).

The **Journal of Biological Research** is, therefore, e-publishing PDF files of an early version of manuscripts that undergone a regular peer review and have been accepted for publication, but have not been through the typesetting, pagination and proofreading processes, which may lead to differences between this version and the final one.

The final version of the manuscript will then appear on a regular issue of the journal.

E-publishing of this PDF file has been approved by the authors.

J Biol Res 2026 [Online ahead of print]

To cite this Article:

Hasan HK, Ali FA, Ahmed GF. **Multi drug control of ESKAPE pathogens by using silver nanoparticles produced by *Pseudomonas putida*.** *J Biol Res* doi: 10.4081/jbr.2026.15666

©The Author(s), 2026

Licensee PAGEPress, Italy

Note: The publisher is not responsible for the content or functionality of any supporting information supplied by the authors. Any queries should be directed to the corresponding author for the article.

All claims expressed in this article are solely those of the authors and do not necessarily represent those of their affiliated organizations, or those of the publisher, the editors and the reviewers. Any product that may be evaluated in this article or claim that may be made by its manufacturer is not guaranteed or endorsed by the publisher.

Submitted: 15 May 2026

Accepted: 23 September 2026

Early access: 13 November 2026

Multi drug control of ESKAPE pathogens by using silver nanoparticles produced by *Pseudomonas putida*

Haveen Khalid Hasan,[1,2] Fattma A. Ali,[3] Ghazwan F. Ahmed[4]

[1]Department of Medical Microbiology, College of Medicine, University of Duhok, Kurdistan Region; [2]Department of Medical Laboratory Technology, College of Health and Medical Technology-Shekan, Duhok Polytechnic University, Duhok, Kurdistan Region; [3]Medical Microbiology Department, College of Health Sciences, Hawler Medical University, Erbil, Kurdistan Region; [4]College of Medicine, University of Duhok, Kurdistan Region, Iraq

Correspondence: Haveen Khalid Hasan, preferred affiliation + shipping address of the affiliation. Tel.: 009647507927306; E-mail: haveen.khalid@dpu.edu.krd

Key words: silver nanoparticles, *Pseudomonas putida*, ESKAPE pathogens, Efflux pump.

Abstract

Despite increasing concerns about antimicrobial resistance among ESKAPE pathogens (*Enterococcus faecium*, *Staphylococcus aureus*, *Klebsiella pneumoniae*, *Acinetobacter baumannii*, *Pseudomonas aeruginosa*, *Enterobacter* spp.), limited studies in Iraq have examined the antimicrobial effects of silver nanoparticles (AgNPs). This study evaluated biogenically synthesized silver nanoparticles using a cell-free extract of *Pseudomonas putida* combined with antibiotics against 83 ESKAPE pathogen isolates and efflux pump activity. The biogenic AgNPs were characterized by Ultraviolet-Visible (UV) spectroscopy, X-Ray Diffractometry (XRD), Fourier Transform Infrared (FT-IR) spectroscopy, Transmission Electron Microscopy (TEM), and Field Emission Scanning Electron Microscopy (FESEM). Combining AgNPs with amoxicillin, nitrofurantoin, levofloxacin, and erythromycin enhanced antibacterial activity

against all tested pathogens. Significant enhancement was observed with erythromycin against *E. faecium* (13.5 mm increase) and amoxicillin against *P. aeruginosa* (16.6 mm increase), and the differences were statistically significant ($p < 0.001$). Efflux pump activity was found in 50/83 (60.2%) isolates, and all 50 (100%) showed enhanced EtBr fluorescence after AgNPs treatment, indicating reduced efflux. This study suggests that AgNPs are efficient antimicrobials and adjuvants against multidrug-resistant (MDR) pathogens. Further investigations are required to determine clinical efficacy and safety.

Introduction

The increasing rate of infections caused by multidrug-resistant bacteria is a major public health concern. According to the Infectious Diseases Society of America (IDSA), the term "ESKAPE pathogens" refers to a group of multidrug-resistant bacteria recognized for their ability to evade the antimicrobial effects of many antibiotics. The ESKAPE pathogens comprise *Enterococcus faecium (E. faecium*), *Staphylococcus aureus* (*S. aureus*), *Klebsiella pneumoniae* (*K. pneumoniae*), *Acinetobacter baumannii* (*A. baumannii*), *Pseudomonas aeruginosa* (*P. aeruginosa*), and *Enterobacter* spp. Such pathogens are referred to as multidrug-resistant bacteria or extensively drug-resistant. They pose a significant risk to patients with weakened immune responses and cause Hospital-Acquired Infections (HAIs), which include most nosocomial infections. The World Health Organization (WHO) identifies ESKAPE as one of 12 bacteria in urgent need of novel medications.[1] The environmental reservoirs of ESKAPE bacteria include aquatic sources, food, soil, vegetation, and domestic waste. All these factors contribute to the emergence of antibiotic resistance.[2] The pathogenic bacteria responsible for antibiotic resistance pose a significant problem in the development of antimicrobial agents.[3] Antimicrobial resistance may lead to the resurgence and development of multi-drug-resistant bacteria.[4] Human pathogen antibiotic resistance is a significant problem in the field of biomedical research and the pharmaceutical industry. Microbial resistance has led to increased hospital stays, mortality and morbidity rates, and costs. To address this issue, scientists have begun researching antimicrobials that could replace or complement antibiotics. One

antimicrobial agent researched is silver nanoparticles (AgNPs), which have proven useful in combating drug-resistant bacteria.[5]

Resistance to antibiotics in bacteria varies. Multidrug-Resistant (MDR) bacteria are isolates that are resistant to at least one drug in three or more classes of antimicrobials. Extensively Drug-Resistant (XDR) bacteria are resistant to at least one drug in all classes of antimicrobials except two or fewer, whereas Pandrug-Resistant (PDR) bacteria are resistant to all antimicrobials. Non-Multidrug-Resistant (non-MDR) isolates are those that do not meet the criteria for multidrug resistance.[6] One of the major factors contributing to antibiotic resistance among bacteria is efflux pumps.[7] Efflux pumps are protein carriers that help get rid of toxins from bacterial cells. Efflux pumps play a key role in drug efflux, making bacteria resistant to antibiotics. Evidence indicates that efflux pumps can have roles in bacteria beyond resistance. These include biofilm formation, pathogenicity, and virulence, showing that efflux pumps affect bacterial physiology in various ways.[8]

Nanotechnology is a promising area for developing innovative material combinations with potential biomedical applications.[9] The cutting-edge field of nanotechnology research includes biology, physics, chemistry, medicine, and materials science.[10] Nanotechnology uses materials less than 100 nanometres (nm).[11] Nanotechnology creates nanostructures with distinct properties. High surface-to-volume ratios affect nanoparticle physicochemical characteristics.[12] They enable many nanometre-scale bioprocesses, making them ideal for biomedical applications.[13] Over the years, Nanoparticles (NPs) like gold (Au), silver (Ag), and magnetic (iron oxide) nanoparticles, as well as nanocages and nanoshells, have been used and modified as therapeutic and diagnostic agents.[14]

However, because of their broad-spectrum antibacterial activity, physicochemical stability, and minimal cytotoxicity at certain concentrations, many scientists have supported the use of AgNPs for biomedical and environmental applications. AgNPs combined with antibiotics offer a unique approach to MDR bacteria management because the synergistic impact of medicines boosts antibacterial effectiveness with less toxicity.[1] *Pseudomonas putida* is a viable biological system for AgNPs biosynthesis because of its metabolic flexibility, stress tolerance, and extracellular enzymatic reduction of Ag^+ ions. Natural reducing and capping agents like reductases and extracellular polymers from bacteria produce well-stabilized nanoparticles with uniform shape, and increased bioactivity.[15] In the present study, biogenically synthesized AgNPs were evaluated,

individually and combined with antibiotics, against ESKAPE pathogens, with a particular focus on disrupting key resistance mechanisms such as efflux pump–mediated drug extrusion.

Materials and Methods

Bacterial culture

This study included 83 clinical isolates of ESKAPE pathogens, comprising: *Enterococcus faecium* (n=17), *Staphylococcus aureus* (n=11), *Klebsiella pneumoniae* (n=24), *Acinetobacter baumannii* (n=12), *Pseudomonas aeruginosa* (n=16), and *Enterobacter* spp. (n=3). The isolates were obtained from urine, blood, wound swabs, sputum, and various clinical specimens collected from patients visiting hospitals in Duhok City, Kurdistan Region, Iraq. *Pseudomonas putida* was isolated from a previously prepared culture and maintained at Duhok Medical Research Center, University of Duhok.

Inclusion and exclusion criteria

The study exclusively incorporated clinical isolates recognized as ESKAPE pathogens. Duplicate isolates from the same patient and non-ESKAPE bacterial strains were excluded.

Antimicrobial susceptibility testing for isolates

Each ESKAPE isolate was tested for antibiotic sensitivity using Mueller-Hinton (MH) agar plates and the disc diffusion method, according to the Clinical and Laboratory Standards Institute (CLSI) procedure.[16] Gram-negative isolates were tested with antibiotic discs containing amoxicillin (30 µg), cefepime (30 µg), ceftriaxone (30 µg), imipenem (10 µg), meropenem (10 µg), ciprofloxacin (5 µg), norfloxacin (10 µg), nitrofurantoin (300 µg), cefixime (5 µg), and amikacin (30 µg). Antibiotics tested for Gram-positive isolates were tetracycline (30 µg), erythromycin (15 µg), Levofloxacin (5 µg), vancomycin (30 µg), teicoplanin (30 µg), linezolid (30 µg), and fusidic acid (10 µg). Isolates were categorized as intermediate, resistant, or susceptible based on the diameter of the inhibitory zone. According to international standards, the isolates were categorized as MDR, XDR, PDR, or non-MDR.[6]

Ethidium bromide (EtBr)-agar cartwheel method (screening method)

The ESKAPE bacterial strains were cultivated in 5 mL of Brain Heart Infusion (BHI) broth at 37°C.[13] MH Agar plates containing 0–2.5 mg/L ethidium bromide (EtBr) were freshly prepared and well protected from light. The plates were divided into radial sectors, and cultures were wiped from the center to the edge. Following 16 hours of dark incubation at 37°C, the plates were observed under a UV transilluminator and photographed (AlphaImager 2200, Alpha Innotech Corporation, San Leandro, CA, USA). The lowest EtBr concentration showing bacterial fluorescence was recorded as indicative of efflux pump activity.[14]

***Biosynthesis of silver nanoparticles by* Pseudomonas putida**

The previously cultured bacterial isolate was cultivated in a 250 mL flask with 100 mL of BHI broth and shaken at 120 rpm at 37°C for 24 hours. To remove cells and prepare extracellular AgNPs, cultures were spun for 10 minutes at 8,000 rpm. After filtering the supernatant, 1 mM $AgNO_3$ was added. The mixture was kept at 25°C and 200 rpm and visually monitored for color change. Incubation was followed by centrifugation at 2,000 rpm for 5 minutes to remove medium debris and at 16,000 rpm for 20 minutes to collect AgNPs. Characterization required multiple water washes and redispersion of the pellet. To make a 10 mg/mL stock solution, the purified AgNPs pellet was suspended in sterile distilled water. Before the bactericidal experiments, AgNPs solutions of 10, 20, 30, and 40 µg/mL were prepared from the stock suspension.[17]

Characterization of silver nanoparticles

Silver nanoparticles (AgNPs) were biosynthesized using cell-free supernatant of *Pseudomonas putida* as described previously. A Ultraviolet-Visible (UV-Vis) spectrophotometer (LAMBDA 35, PerkinElmer Inc., Waltham, MA, USA) was used to confirm silver ion reduction and nanoparticle production at 200–800 nm. X-ray diffraction (XRD) was used to define the crystalline structure of the biosynthesized AgNPs. The working parameters were: 40 kV, 40 mA, and a wavelength of 0.15406 nm.[18] XRD (PW 1730, Philips, Eindhoven, The Netherlands) patterns were scanned using a 2θ scale from 20° to 80° at 6°/min with a step size of 0.02°. The average crystallite size was calculated using the Scherrer equation, $D=K\lambda/\beta\cos\theta$, where D is the crystallite size, K=0.9, λ=0.15406 nm, β is the Full Width at Half Maximum (FWHM) of the diffraction peak in radians, and θ is the Bragg angle. The biomolecules used in order to reduce

and cap AgNPs were discovered by Fourier-Transform Infrared (FTIR) spectroscopy (LAMBDA 35, PerkinElmer Inc., Waltham, MA, USA).[19]

AgNPs were characterized by Transmission Electron Microscopy (TEM) and Field-Emission Scanning Electron Microscopy (FESEM) (PW 1730, Philips, Eindhoven, The Netherlands) to assess nanoparticle size, morphology, and distribution. The TEM analysis included placing a drop of the solution on a carbon-coated copper grid and air-drying at 60°C. Quantitative TEM analysis of 203 nanoparticles using ImageJ /Fiji (v1.54) determined the mean size, Standard Deviation (SD), size distribution, and TEM-derived PDI (PDI_TEM). FESEM was used to characterize nanoparticle surface morphology.[20,21]

Application of AgNPs in the cartwheel EtBr assay

Efflux pump inhibition by AgNPs was evaluated using the cartwheel assay with EtBr. Initial testing showed that at AgNPs concentrations of 1–5 µg/mL, fluorescence remained inhibited, while at 10 µg/mL it became more apparent. Isolates were streaked onto agar containing 0.5–2.5 mg/L EtBr and incubated in the dark at 37°C for 16 hours. Enhanced fluorescence under UV illumination following AgNPs treatment was interpreted as increased intracellular EtBr accumulation and reduced efflux activity.[22]

Antibacterial activity of AgNPs combined with antibiotics

The disc diffusion and agar well diffusion methods were used to evaluate the antibacterial efficacy of biogenic AgNPs, antibiotics alone, and in combination against bacterial isolates, according to Sundar et al.[1] After adjusting the bacterial suspension in MH broth to a 0.5 McFarland standard (approximately 1.5×10^8 Colony-Forming Units (CFU)/mL), the suspension was inoculated onto MH agar plates.[23] The agar-well diffusion method was used to assess the concentration-dependent antibacterial activity of AgNPs solutions (10, 20, 30, and 40 µg/mL). In the combination assay, 20 µg/mL was chosen as the lowest concentration that produced detectable inhibitory zones against the tested isolates. After 24 h of incubation, the inhibition zone diameters were measured in millimeters, and the percentage fold increase was calculated by comparing the combinations with the antibiotics alone. Each combination assay was performed in triplicate, and the results are presented as the mean ± SD. Antimicrobial susceptibility was interpreted according to the Clinical and Laboratory Standards Institute (CLSI) guidelines.[16]

Statistical analysis

Data were analyzed using the Statistical Package for Social Sciences 27 (SPSS 27; IBM Corp., Armonk, NY, USA). Descriptive findings were presented in frequencies and percentages. The means of the diameter of inhibition zones for standard antibiotics were compared using a paired-sample t-test. Associations between categories were analyzed using the Fisher-Freeman-Halton exact test. A p value of < 0.05 was considered statistically significant.

Results

Distribution of MDR, XDR, PDR, and Non-MDR ESKAPE pathogens among patients

Table 1 shows the prevalence of MDR, XDR, PDR, and non-MDR ESKAPE pathogens that were isolated during this study.

Among the ESKAPE pathogens examined, MDR isolates predominated, with *Enterococcus faecium* showing the highest prevalence (70.5%). PDR isolates were the next most common, primarily in *Acinetobacter baumannii* (50%), followed by XDR, which were also identified in *Acinetobacter baumannii* (25%). Non-MDR isolates were identified in *Enterobacter* spp. (33.3%). Statistically significant differences in MDR, XDR, PDR, and Non-MDR were observed among the ESKAPE bacteria (p value < 0.001).

Distribution of efflux pump activity among ESKAPE pathogens

The EtBr agar cartwheel assay was used as a screening method to assess EtBr accumulation, which may indicate altered efflux activity in ESKAPE isolates. Of the 83 isolates examined, 50 (60.2%) were efflux-pump positive, while 33 (39.7%) were negative. The highest prevalence of efflux-pump activity was observed in *Enterococcus faecium* (100%), whereas the lowest prevalence was observed in *Klebsiella pneumoniae* (29.1%). Efflux-pump activity differed significantly among the tested ESKAPE species ($p = 0.001$; Table 2; Figure 1A).

Synthesis of silver nanoparticles using **Pseudomonas putida**

Using *Pseudomonas putida* supernatant, the silver nanoparticles were synthesized biologically. The silver nitrate flask changed from yellow to brown, indicating silver nanoparticle formation, whereas the control and blank flasks did not change color.

Characterization of AgNPs

Ultraviolet-Visible (UV-Vis) Spectral analysis

A UV-Vis spectrophotometer (LAMBDA 35, PerkinElmer Inc., Waltham, MA, USA) was used to analyze the AgNPs reaction mixture. The incubated reaction mixture was scanned at 200–800 nm. AgNPs' surface plasmon resonance band causes the intense UV-Vis absorption peak at 415 nm. This band appears to be the silver nanoparticle surface plasmon resonance. Thus, the reaction mixture shows AgNPs (Figure 2A).

X-ray diffraction

XRD analysis confirmed the crystalline nature of the biosynthesized AgNPs. Distinct diffraction peaks were observed at approximately 28°, 33°, 39°, 47°, 55°, 58°, 68°, 75°, and 77° (2θ), indicating the presence of crystalline silver along with silver oxide phases (Figure 2B). The average crystallite size, calculated using the Scherrer equation, was approximately 16.8 nm, confirming the nanocrystalline nature of the biosynthesized AgNPs. A broad amorphous background was also observed, which may be linked to organic biomolecules from *Pseudomonas putida* acting as reducing, capping, and stabilizing agents.

Fourier Transform-Infrared (FT-IR) spectroscopy

Biosynthesized AgNPs showed typical FTIR peaks, confirming biomolecules on their surface. Broad bands at 3,200 and 3,500 cm^{-1} suggest O-H and N-H stretching, whereas a peak at 1,600 cm^{-1} shows C=O and C=N groups. Additional peaks at 1,300-1,400 cm^{-1} and 1,000-1,100 cm^{-1} are C-N and C-O stretching peaks. These functional groups show that bacterial metabolites reduced and stabilized AgNPs biosynthesis (Figure 2C).

Field Emission Scanning Electron Microscopy (FESEM)

FESEM examined the morphology of AgNPs. The FESEM image revealed mostly spherical particles. The particles were associated in close groups, displaying characteristics of the synthesized AgNPs (Figure 2D).

Transmission Electron Microscopy (TEM)

TEM analysis was carried out to determine the morphology and particle-size distribution of the synthesized AgNPs. TEM revealed spherical nanoparticles predominantly arranged in clusters. Particle-size analysis of 203 nanoparticles showed a mean diameter of 44.9 ± 26.23 nm and a median diameter of 37.75 nm, with sizes ranging from 10.77 to 149.63 nm. The particle-size histogram showed a broad distribution with a clear dominant peak, indicating a major particle-size population. The PDI_TEM was 0.341, indicating particle-size heterogeneity. Generally, TEM confirmed the nanoscale size and spherical morphology of the AgNPs (Figure 2E).

Analysis of antimicrobial activity of AgNPs

Using agar-well diffusion, the synthesized AgNPs showed concentration-dependent antibacterial activity against all tested isolates. At 10 µg/mL, no inhibition zones were found, indicating ineffectiveness against all tested isolates. The antibacterial activity was visible at 20 µg/mL, with measurable inhibition zones across the bacterial panel. The inhibitory effect increased significantly at 30 µg/mL, resulting in larger zone widths than at 20 µg/mL. The maximum antibacterial activity was obtained at 40 µg/mL, with the largest inhibition zones for all tested strains. Thus, 20 µg/mL can be considered the minimum concentration exhibiting measurable antibacterial effects.

Application of silver nanoparticles on activity of the Efflux pump

The cartwheel assay was employed to assess the efflux pump-inhibiting activity of the synthesized AgNPs. The 50 efflux-pump-positive isolates were evaluated following exposure to biogenic AgNPs. Following AgNPs treatment, all 50 isolates (100%) showed enhanced EtBr fluorescence, indicating increased intracellular EtBr accumulation and suggesting reduced efflux activity (Figure 1B).

Efficacy of tested nanoparticles on enhancing the activity of different antibiotics

The disc diffusion method was used to evaluate the antibacterial activity of antibiotics alone and in combination with silver nanoparticles (AgNPs) against the tested bacteria. AgNPs enhanced antibiotic effectiveness against both Gram-positive and Gram-negative ESKAPE strains. *E. faecium* had the largest zone of inhibition for Erythromycin (E) at 13.5 mm among Gram-positive bacteria. *P. aeruginosa* had the highest amoxicillin enhancement of 16.55 mm among

Gram-negative bacteria. Table 3 shows that AgNPs enhanced antibiotic antibacterial activity. Combining antibiotics with AgNPs statistically significantly enhanced antibacterial activity against all ESKAPE isolates; *Enterobacter* spp. was the only exception.

Discussion

The emergence and re-emergence of Multidrug-Resistant (MDR) pathogenic bacteria have become major public health challenges over the past decade.[1] MDR bacteria are a significant public health problem due to their increased resistance to existing antibiotics. The ESKAPE pathogens (*Enterococcus faecium*, *Staphylococcus aureus*, *Klebsiella pneumoniae*, *Acinetobacter baumannii*, *Pseudomonas aeruginosa*, and *Enterobacter* spp.) are especially important because they cause most hospital-acquired infections and have multiple antimicrobial resistance mechanisms. Globally and locally, infections caused by ESKAPE pathogens are associated with extended hospital stays, increased mortality, higher healthcare costs, and limited therapeutic options.[24]

Most ESKAPE pathogens in this study were MDR, followed by PDR and XDR. The main MDR strains included *E. faecium,* while PDR and XDR strains included *Acinetobacter baumannii.* These findings align with previous literature identifying high rates of antimicrobial resistance in ESKAPE pathogens. In the present study, multidrug resistance was found in *E. faecium* isolates, owing to the ability of this bacterium to acquire multiple resistance mechanisms and survive antimicrobial selective pressure. In addition, Aziz and Alabdali mentioned high rates of antimicrobial resistance among the clinical *E. faecium* isolates from Al-Muthanna Province, Iraq.[25] Moreover, in the current study, XDR and PDR phenotypes were also noted among *A. baumannii* isolates. This bacterium can acquire different resistance mechanisms, form biofilms, and survive in hospital settings, thus causing the development and spread of the most resistant strains. Furthermore, Alabdali[26] found highly antibiotic-resistant *A. baumannii* isolates in Al-Muthanna Province, Iraq; they also detected class I integrons associated with antimicrobial resistance.[26] Statistical analysis demonstrated a significant difference in the distribution of resistance patterns among ESKAPE pathogens ($p < 0.001$), indicating species-specific variation in resistance phenotypes. This finding highlights the heterogeneity of antimicrobial resistance among the investigated ESKAPE pathogens and may reflect differences in their intrinsic and acquired resistance characteristics.

The EtBr cartwheel assay showed considerable variation in efflux activity among ESKAPE pathogens, with a significant difference among species ($p < 0.001$), indicating species-dependent variation in the efflux phenotype. As the EtBr cartwheel assay is an indirect screening method, fluorescence patterns may reflect not only efflux activity but also factors affecting EtBr accumulation, including membrane permeability, membrane integrity, and the proton motive force.

Various studies from Iraq have shown similar resistance traits. Ganjo *et al.*[27] reported high carriage rates of efflux and porin-associated genes, such as *acrAB* and *ompF*/*ompC* genes, in clinical *Escherichia coli* isolates in Erbil. Hussein *et al*.[28] found *acrAB* and *tolC* efflux pump genes in over 90% of multidrug-resistant *Klebsiella pneumoniae* isolates in Al-Anbar, and porin genes *ompK35* and *ompK36* in 80% of isolates. These reports support the contribution of efflux systems and altered outer-membrane permeability to antimicrobial resistance among clinical Gram-negative isolates in Iraq.

This study biosynthesized AgNPs using a cell-free *Pseudomonas putida* extract as a reducing agent. Biogenic reduction converted silver ions (Ag^{+}) into elemental silver (Ag^{0}).[29] The characteristic color change of the reaction medium from pale yellow to brown, which is associated with surface plasmon resonance of AgNPs, confirmed the synthesis. These results are consistent with those published in Ukraine by Plokhovska *et al.*[17]

AgNPs synthesis was further supported by UV–Visible spectroscopy, which showed a particular surface plasmon resonance (SPR) peak at 415 nm. In Egypt, UV-Visible spectroscopy confirmed AgNPs synthesis using *Bacillus velezensis* BS1 biosynthesis. Sharp SPR peaks were observed at 410-450 nm, showing small and dispersed nanoparticles.[30]

FESEM and TEM analyses showed that the synthesized AgNPs were mostly spherical, confirming successful formation of nanoscale silver particles. Similar morphological characteristics were reported by Shamsoddini *et al*., who observed spherical AgNPs by SEM with particle sizes ranging from 10 to 130 nm and a mean size of 38.89 nm.[31] TEM analysis in the present study revealed a mean particle diameter of 44.92 ± 26.23 nm, further confirming the nanoscale dimensions of the synthesized AgNPs. This finding is comparable to that of Allafchian et al., who reported spherical AgNPs with a mean TEM diameter of approximately 45 nm and demonstrated their antibacterial activity.[32] The close agreement with previously reported

biologically synthesized AgNPs supports the characteristic morphology and nanoscale dimensions of the AgNPs obtained in the present study.

X-ray diffraction revealed sharp peaks for metallic silver with a face-centered cubic crystal structure, indicating high purity and crystallinity. Similar XRD patterns have been reported by Ali *et al.*,[33] who also observed characteristic diffraction peaks corresponding to the face-centered cubic crystal structure of metallic silver.

FTIR analysis indicated amide, hydroxyl, and carbonyl group peaks, suggesting the reduction and stabilization of nanoparticles by bacterial proteins and other biomolecules. Pasieczna-Patkowska *et al.* (Poland) also reported amide, hydroxyl, and carbonyl peaks, indicating reduction and stabilization of AgNPs by bacterial proteins and biomolecules.[34] These functional groups may function as reducing and capping agents and may affect nanoparticle stability and interactions with bacterial cells.

Biologically produced nanoparticles are polydisperse because they have lower control over nucleation and growth than chemically or physically synthesized ones. Biosynthesis of nanoparticles involves bacterial enzymes and NADPH-dependent reductases reducing silver ions (Ag^{+} to Ag^{0}), stabilizing them through the capping effect. This process is similar to those described by Sharmin *et al.*[35] and by Singh and Gupta.[36] The biosynthesis of nanoparticles in these studies produced polydisperse nanoparticles by reducing silver ions (Ag^{+} to Ag^{0}) with bacterial enzymes and NADPH-dependent reductases, stabilizing them with biomolecules.[35,36]

In the present study, biogenic AgNPs enhanced the antibacterial activity of several antibiotics against ESKAPE pathogens, as demonstrated by increased inhibition zone diameters in the disc diffusion assay. Combining AgNPs with various antibiotics increased inhibition zones against all ESKAPE pathogens tested. Statistical analysis confirmed that this improvement was significant compared with antibiotics alone, supporting the potentiating effect of AgNPs on antibiotic activity. *Enterobacter* spp. was the only exception, which may be attributed to the small number of isolates.

Specifically, combining AgNPs with amoxicillin and nitrofurantoin showed enhanced antibacterial activity against Gram-negative bacteria, which may be attributed to their ability to alter bacterial membrane permeability. Consistent with the results obtained in the present study, Tawfeeq *et al.*[37] found enhanced antibacterial effects of AgNPs in combination with tobramycin, chloramphenicol, nitrofurantoin, amoxicillin-clavulanic acid, and nalidixic acid against

multidrug-resistant bacteria in Iraq. Gram-positive bacteria showed greater enhancement, especially with levofloxacin and erythromycin. This agrees with earlier studies indicating that AgNPs improve antibiotic delivery.[23,38] Similarly, Fareid *et al.*[39] found enhanced antibacterial effect of erythromycin in combination with AgNPs against methicillin-resistant *Staphylococcus aureus*.

In the current study, combining antibiotics with AgNPs substantially enhanced antibacterial activity against ESKAPE isolates. This effect may be linked to the ability of AgNPs to regulate the integrity and permeability of bacterial membranes, thereby facilitating the entry of antibiotics into bacterial cells.

Furthermore, AgNPs treatment increased EtBr fluorescence in previously non-fluorescent isolates, indicating greater intracellular EtBr accumulation consistent with reduced efflux activity. Similarly, El-Deeb *et al.*[22] reported increased EtBr accumulation after AgNPs treatment of resistant *P. aeruginosa*, suggesting efflux pump inhibition. Attallah *et al.*[40] also reported reduced efflux activity in *S. aureus* isolates following treatment with AgNPs.

Some experimental groups had substantial standard deviations, perhaps due to clinical isolate variability. Variability in antibacterial susceptibility may reflect antimicrobial resistance determinants, efflux pump activity, biofilm formation, and prior antibiotic exposure. Given the range of clinical isolates and resistance characteristics, this variability is expected.

Current research was carried out *in vitro* on a limited number of isolates, and antibacterial activity was assessed by disc diffusion without determining Minimum Inhibitory Concentration (MIC) and Minimum Bactericidal Concentration (MBC) values. Cytotoxicity and anti-biofilm activities were not explored either. Future work should include such tests to assess the effectiveness of AgNPs as medicine.

Conclusions

Biogenic AgNPs exhibited dose-dependent antibacterial activity against the tested bacterial isolates, including ESKAPE pathogens. In addition, AgNPs enhanced the antibacterial activity of several antibiotics against these pathogens under *in vitro* conditions, as demonstrated by increased inhibition zones in the disc diffusion assay. These findings suggest that biogenic AgNPs may serve as a promising adjunct to conventional antibiotics for fighting antimicrobial-

resistant bacteria. Further studies are required to confirm their efficacy, safety, and clinical applicability before clinical or veterinary use.

References

1. Sundar PS, Musoliwa R, Kondiah K. Novel biogenic silver nanoparticles produced by *Enterobacter xiangfangensis* Pb204 reinstate the activity of specific antibiotics against resistant ESKAPE pathogens. Nanoscale Adv 2026;8:701-11.
2. Mabeo OR, Tsholo K, Bezuidenhout CC, Molale-Tom LG. Comparison of ESKAPE pathogen levels in wastewater and receiving water bodies using agar-based enumeration and real-time PCR. Curr Microbiol 2026;83:128.
3. Khairnar SV, Das A, Oupický D, et al. Strategies to overcome antibiotic resistance: silver nanoparticles and vancomycin in pathogen eradication. RSC Pharm 2025;2:455-79.
4. El-Saadony MT, Saad AM, Mohammed DM, et al. Medicinal plants: bioactive compounds, biological activities, combating multidrug-resistant microorganisms, and human health benefits: a comprehensive review. Front Immunol 2025;16:1491777.
5. Khalifa HO, Oreiby A, Mohammed T, et al. Silver nanoparticles as next-generation antimicrobial agents: mechanisms, challenges, and innovations against multidrug-resistant bacteria. Front Cell Infect Microbiol 2025;15:1599113.
6. Magiorakos AP, Srinivasan A, Carey RB, et al. Multidrug-resistant, extensively drug-resistant and pandrug-resistant bacteria: an international expert proposal for interim standard definitions for acquired resistance. Clin Microbiol Infect 2012;18:268-81.
7. Husain MF, Kandala NJ. Molecular and phenotypic characterization of efflux pumps and efflux pump inhibitors on antibiotic resistance of *Salmonella* Typhi in Baghdad. Iraq J Agric Sci 2025;56:755-66.
8. Nasir AA, Al-Mousawi AA, Abdul-Hussein ZR. Detection of AcrAB efflux pumps gene, biofilm formation in *Escherichia coli* and *Klebsiella pneumoniae* isolated from pregnant women with urinary tract infections and diabetes mellitus in Basrah City, Iraq. Rev Diabet Stud 2025;21:297.

9. Hosny S, Mohamed LZ, Ragab MS, et al. Nanomaterials in biomedical applications: opportunities and challenges—a review. Chem Pap 2025;79:2657-78.
10. John J. Cutting-edge nanoparticle innovations in biomedical science: synthesis, applications, challenges, and future prospects. J Nanotechnol Nanomater 2025;6:43-66.
11. Deleanu L, Popa C, Ojoc GG, et al. Terminology and standards in research at nano level. J Eng Sci Innov 2025;10:103-30.
12. Anandhan A, Bansod PJ. *Nanotechnology in the 21st century: innovation and challenges.* New Delhi: Addition Publishing House; 2025.
13. Abdel-Mageed HM. Frontiers in nanoparticles redefining enzyme immobilization: a review addressing challenges, innovations, and unlocking sustainable future potentials. Micro Nano Syst Lett 2025;13:7.
14. Singh P, Pandit S, Balusamy SR, et al. Advanced nanomaterials for cancer therapy: gold, silver, and iron oxide nanoparticles in oncological applications. Adv Healthcare Mater 2025;14:2403059.
15. Thamilselvi V, Radha KV. Synthesis of silver nanoparticles from *Pseudomonas putida* NCIM 2650 in silver nitrate supplemented growth medium and optimization using response surface methodology. Dig J Nanomater Bios 2013;8:1101-11.
16. Clinical and Laboratory Standards Institute. Performance standards for antimicrobial susceptibility testing. 34th ed. CLSI supplement M100. Wayne, PA: Clinical and Laboratory Standards Institute; 2024.
17. Plokhovska S, Fuente-González E, Gutierrez-Albanchez E, et al. AgNPs biosynthesized from *Pseudomonas* Z9.3 metabolites as antimicrobial agents against bacterial and fungal pathogens. Front Microbiol 2025;16:1565689.
18. Abu-Hussien SH, Khan MA, Al-Farga A, et al. Biogenic silver nanoparticles synthesized from *Pseudomonas fluorescens*-mediated olive cake waste: antimicrobial, larvicidal activity against *Culex pipiens* and cytotoxicity assessment. BMC Biotechnol 2025;25:75.
19. Jose A, Asha S, Rani A, Xavier TS, Kumar P. *Pseudomonas otitidis*-mediated synthesis of silver nanoparticles: characterization, antimicrobial and antibiofilm potential. Lett Appl Microbiol 2024;77.
20. Jan S, Jan N, Singh S, Shah MA, Malik MA. Crystalline defenders: silver nanoparticles as a new front in antimicrobial warfare. Curr Res Green Sustain Chem 2025;5:100481.

21. Mohammed ABA, Abd Elhamid MM, Khalil MKM, et al. The potential activity of biosynthesized silver nanoparticles of *Pseudomonas aeruginosa* as an antibacterial agent against multidrug-resistant isolates from intensive care unit and anticancer agent. Environ Sci Eur 2022;34:109.
22. El-Deeb NM, Abo-Eleneen MA, Al-Madboly LA, et al. Biogenically synthesized polysaccharides-capped silver nanoparticles: immunomodulatory and antibacterial potentialities against resistant *Pseudomonas aeruginosa*. Front Bioeng Biotechnol 2020;8:643.
23. AlQurashi DM, AlQurashi TF, Alam RI, et al. Advanced nanoparticles in combating antibiotic resistance: current innovations and future directions. J Nanotheranostics 2025;6:9.
24. Álvarez-Ainza ML, Fong-Coronado PA, Ruiz-Bustos E, et al. Antibiotic resistance of ESKAPE group-microorganisms in health institutions from Hermosillo and Ciudad Obregón, Sonora, México. Front Cell Infect Microbiol 2024;14:1348093.
25. Aziz ZN, Alabdali YAJ. Characterisation of antibiotic resistance pattern of *Enterococcus faecalis* and *Enterococcus faecium* isolated from different clinical specimen in Al-Muthanna Province, Iraq. J Wasit Sci Med 2024;17:76-88.
26. Alabdali YAJ. Antibiotic resistance and carriage class I integron in clinical isolates of *Acinetobacter baumannii* from Al Muthanna, Iraq. J Antibiot (Tokyo) 2022;75:691-7.
27. Ganjo AR, Balaky STJ, Mawlood AH, et al. Characterization of genes related to the efflux pump and porin in multidrug resistant *Escherichia coli* strains isolated from patients with COVID-19 after secondary infection. BMC Microbiol 2024;24:122.
28. Hussein RA, Al Kubaisy SH, Al Ouqaili MTS. The influence of efflux pump, outer membrane permeability and β-lactamase production on the resistance profile of multidrug-, extensively drug-, and pandrug-resistant *Klebsiella pneumoniae*. J Infect Public Health 2024;17:102544.
29. Cruz Romero CL, Chávez Ramírez AU, Flores Juárez CR, et al. Biosynthesis of polyhydroalkanoates doped with silver nanoparticles using *Pseudomonas putida* and *Pseudomonas aeruginosa* for antibacterial polymer applications. Int J Mol Sci 2024;25:8996.

30. Aletrepy AA, Selim AEI, Ashour EH, Omar SA. Green synthesis of silver nanoparticles by isolated *Bacillus velezensis* BS1 and their applications. Appl Microbiol Biotechnol 2026;110:70.
31. Shamsoddini SM, Davoudi M, Shahbazi S, Zare Karizi S. Green synthesis of silver nanoparticles using *Acroptilon repens* aqueous extract and their antibacterial efficacy against multidrug-resistant Acinetobacter baumannii. Mol Biol Rep 2024;52:47.
32. Allafchian AR, Jalali SAH, Aghaei F, Farhang HR. Green synthesis of silver nanoparticles using *Glaucium corniculatum* (L.) Curtis extract and evaluation of its antibacterial activity. IET Nanobiotechnol 2018;12:574-8.
33. Ali IF, Al Joboory RKI, Al Shammari HI. Evaluating the efficiency of silver nanoparticles prepared using *Pseudomonas fluorescens* and *Bacillus thuringiensis* subsp. *tenebrionis* in controlling eggs and adults of *Callosobruchus maculatus* (F.) (Coleoptera: Bruchidae). J Biol Control 2024;38:29-40.
34. Pasieczna Patkowska S, Cichy M, Flieger J. Application of Fourier transform infrared (FTIR) spectroscopy in characterization of green synthesized nanoparticles. Molecules 2025;30:684.
35. Sharmin S, Islam MB, Saha BK, et al. Evaluation of antibacterial activity, *in vitro* cytotoxicity and catalytic activity of biologically synthesized silver nanoparticles using leaf extracts of *Leea macrophylla*. Heliyon 2023;9:e20810.
36. Singh K, Gupta V. Field emission scanning electron microscopic, X-ray diffraction and ultraviolet spectroscopic analysis of *Terminalia bellerica*-based silver nanoparticles and evaluation of their antioxidant, catalytic and antibacterial activity. Heliyon 2023;9:e16944.
37. Tawfeeq SM, Maaroof MN, Al Ogaidi I. Synergistic effect of biosynthesized silver nanoparticles with antibiotics against multidrug-resistant bacteria isolated from children with diarrhoea under five years. Iraq J Sci 2017;58:14-52.
38. Adebayo EA, Ibikunle JB, Oke MA, et al. Antimicrobial and antioxidant activity of silver, gold, and silver-gold alloy nanoparticles phytosynthesized using extract of *Opuntia ficus-indica*. Rev Adv Mater Sci 2019;58:313-26.

39. Fareid MA, El Sherbiny GM, Askar AA, et al. Impeding biofilm-forming mediated methicillin-resistant *Staphylococcus aureus* and virulence genes using a biosynthesized silver nanoparticles-antibiotic combination. Biomolecules 2025;15:266.
40. Attallah NGM, Elekhnawy E, Negm WA, et al. *In vivo* and *in vitro* antimicrobial activity of biogenic silver nanoparticles against *Staphylococcus aureus* clinical isolates. Pharmaceuticals (Basel) 2022;15:194.

Table 1. Prevalence of Multidrug-Resistant (MDR), Extensively Drug-Resistant (XDR), Pandrug-Resistant (PDR), and Non-Multidrug-Resistant (non-MDR) phenotypes among ESKAPE bacteria.

Organism	**Total n**	**MDR n (%)**	**XDR n (%)**	**PDR n (%)**	**Non- MDR n (%)**	**p value**
Enterococcus faecium	17	12 (70.5)	4 (23.5)	1 (5.8)	0 (0)	
Staphylococcus aureus	11	7 (63.6)	2 (18.1)	0 (0)	2 (18.1)	
Klebsiella pneumoniae	24	14 (58.3)	3 (12.5)	2 (8.3)	5 (20.8)	
Acinetobacter baumannii	12	1 (8.3)	3 (25)	6 (50)	2 (16.6)	< 0.001
Pseudomonas aeruginosa	16	11 (68.7)	1 (6.2)	4 (25)	0 (0)	
***Enterobacter* spp.**	3	1 (33.3)	0 (0)	1 (33.3)	1 (33.3)	
Total	83	46 (55.4)	13 (15.6)	14 (16.8)	10 (12)	

Table 2. Distribution of organisms among the isolates.

Organism	**n of isolates**	**Efflux Pump positive n (%)**	**Efflux Pump negative n (%)**	**p value**
Enterococcus faecium	17	17 (100)	0 (0)	< 0.001

Staphylococcus aureus	11	9 (81.8)	2 (18.1)
Klebsiella pneumoniae	24	7 (29.1)	17 (70.8)
Acinetobacter baumannii	12	9 (75)	3 (25)
Pseudomonas aeruginosa	16	6 (37.5)	10 (62.5)
***Enterobacter* spp.**	3	2 (66.6)	1 (33.3)
Total	83	50 (60.2)	33 (39.7)

Table 3. Antibacterial activity (inhibition zone in mm) of biogenic silver nanoparticles (AgNPs) against ESKAPE pathogens. Mean zone of inhibition (mm) ± standard deviation (SD) of AgNPs at different concentration against ESKAPE isolates (each measured in triplicate).

No. of Microorganism	**(20 µg/mL)**
Enterococcus faecium	16.67 ± 0.58
Staphylococcus aureus	16.33 ± 0.58
Klebsiella pneumoniae	14.33 ± 0.58
Acinetobacter baumannii	14 ± 0.58
Pseudomonas aeruginosa	13.33 ± 0.58
***Enterobacter* spp.**	14.33 ± 0.58

Table 4. Mean diameters of inhibition zones of antibiotics (Ab.) against ESKAPE isolates, alone and in combination with silver nanoparticles (AgNPs), with 95% confidence interval (CI).

	Ab. Combine with AgNPs (Mean)				
Name of	**Ab. zones of**	**zones of**	**Increase**	**p value**	**95% CI**

Bacteria		**inhibition (mm)**	**inhibition with AgNPs (mm)**	**(mm)**		
Enterococcus faecium	LEV	10.7 ± 6.02	23.1 ± 4.12	12.4	<0.001	9.180-15.643
	E	6.1 ± 6.69	19.6 ± 2.55	13.5	<0.001	9.941- 17.001
Staphylococcus aureus	LEV	11.4 ± 5.99	20.2 ± 3.33	8.8	0.00015	5.599-12.038
	E	9.4 ± 7.07	19.4 ± 3.27	10.0	0.00017	6.382- 13.618
Klebsiella pneumoniae	AM	3.8 ± 6.21	17.7 ± 3.71	13.9	<0.001	12.208- 15.542
	F	9.2 ± 6.89	18.9 ± 2.73	9.7	0.000001	6.632- 12.785
Acinetobacter baumannii	AM	1.5 ± 4.74	17.5 ± 3.06	16.0	<0.001	12.995- 19.005
	F	1.5 ± 4.74	17 ± 3.02	15.5	<0.001	12.132- 18.868
Pseudomonas aeruginosa	AM	1.45 ± 4.82	18 ± 2.76	16.55	<0.001	13.204-19.921
	F	5 ± 6.73	18.5 ± 2.95	13.5	<0.001	10.825- 16.175
***Enterobacter* spp.**	AM	5 ± 8.66	20.7 ± 2.08	15.7	0.055	0.875- 32.270
	F	5 ± 8.66	18.7 ± 1.15	13.7	0.08	4.978- 32.311

LEV, levofloxacin; E, erythromycin; AM, amoxicillin; F, nitrofurantoin.

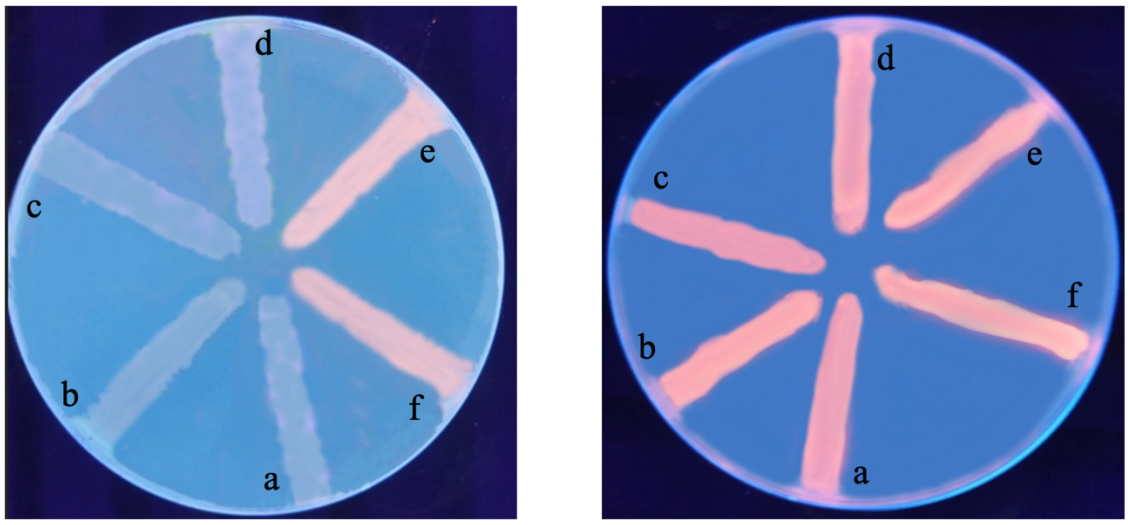

A: Efflux activity before AgNPs treatment B: Efflux activity after AgNPs treatment

Figure 1. Phenotypic efflux pump activity and inhibitory effect of silver nanoparticles (AgNPs) assessed by the ethidium bromide (EtBr)-agar cartwheel assay: (A) EtBr-agar without silver nanoparticles (AgNPs), (a–d) positive efflux pump activity indicate by the absence of fluorescence (e–f) negative efflux pump activity, indicate by the presence of fluorescence; (B) EtBr-agar supplemented with 10 µg/mL of silver nanoparticles (AgNPs), (a–f) showing fluorescence, indicating inhibition of efflux pump activity by AgNPs.

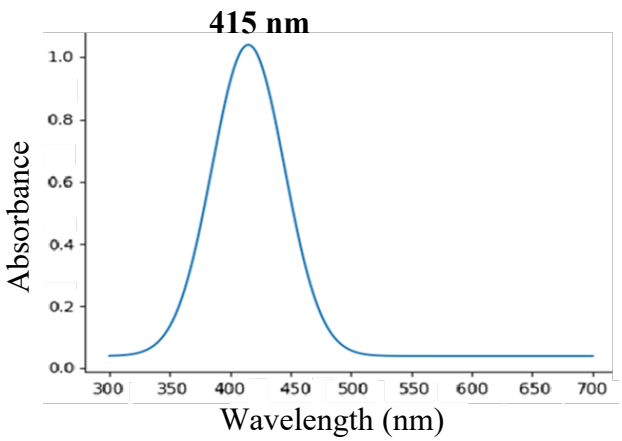

A) UV-Vis

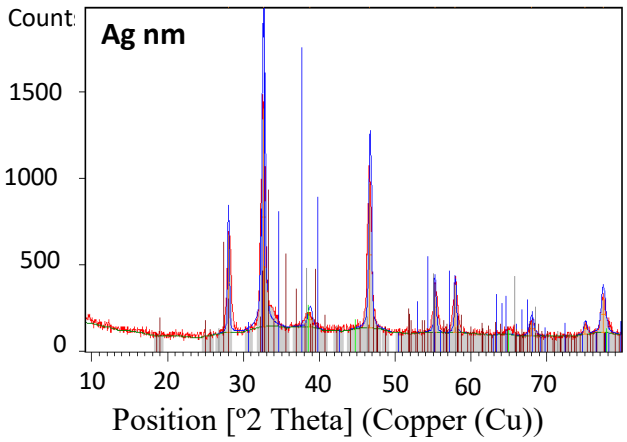

B) XRD

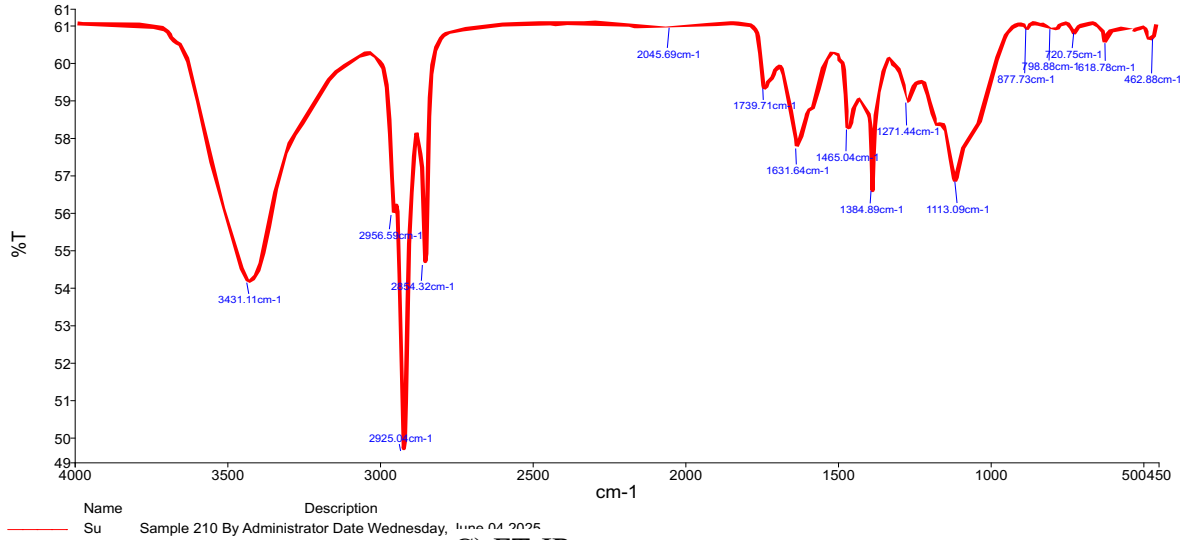

C) FT-IR spectroscopy

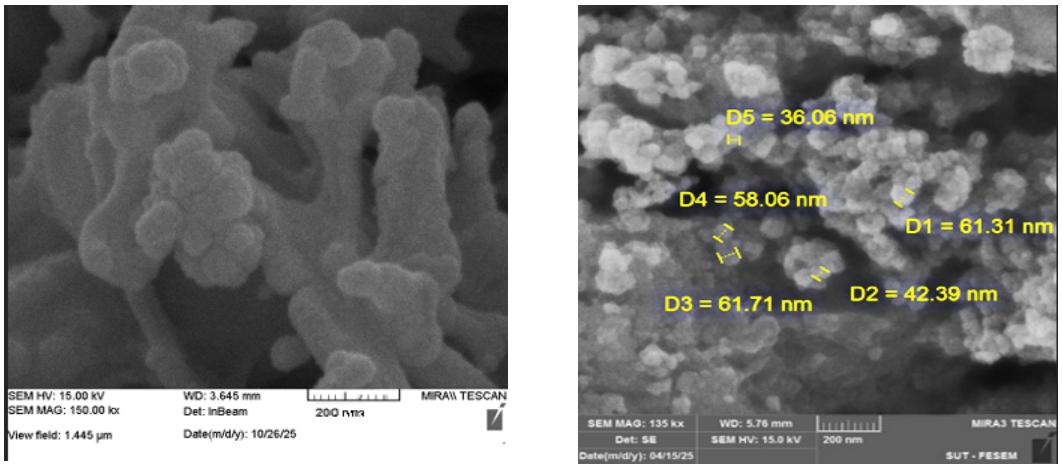

D) FESEM

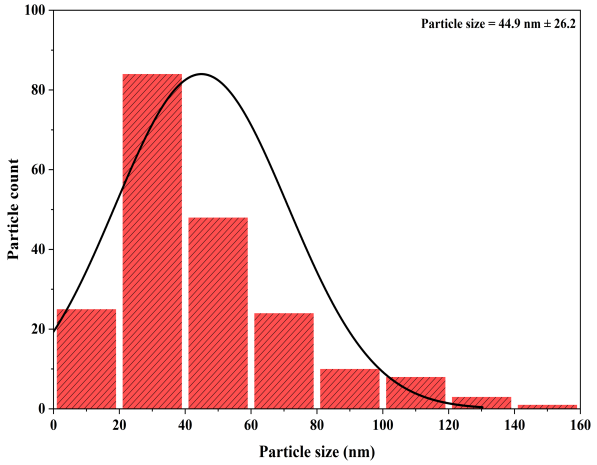

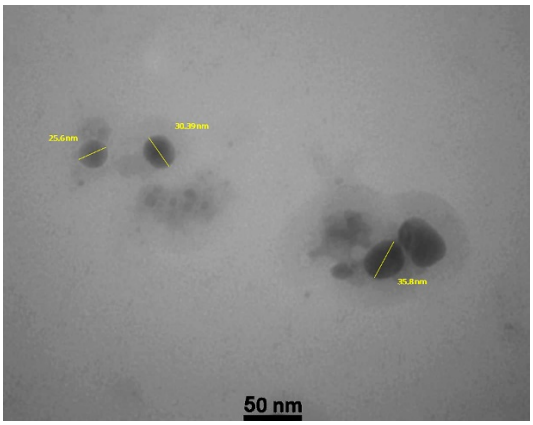

E) Histogram of size dispersion and TEM

Figure 2. Characterization of silver nanoparticles (AgNPs) synthesized by *Pseudomonas putida*: (A) Ultraviolet-visible (UV-Vis) Spectral analysis, (B) X-ray diffraction (XRD), (C) Fourier transform-infrared (FT-IR) spectroscopy, (D) Field Emission Scanning Electron Microscopy (FESEM), and (E) Transmission Electron Microscopy (TEM) image with corresponding particle -size distribution histogram.

Contributions: Haveen Khalid Hasan developed the study, did the lab experiments, evaluated the data, prepared the figures and tables, and drafted the report. The co-authors contributed to the supervision, critical editing of the article, and approval of the final version. All authors have read and approved the final manuscript.

Conflict of interest: no conflict of interest is declared.

Ethics statement: this study was approved by the Research Ethics Committee of Duhok Directorate General of Health (Date: 29 May 2024; Reference No.: 29052024-4-19).

Patient consent: written informed consent for both participation in the study and publication of the results was obtained from the patients or their guardians.

Data availability statement: data underlying this study can be obtained from the corresponding author upon reasonable request.

Funding: none.

AI use statement: the authors declare the use of AI (ChatGPT) to rephrase and enhance the clarity of the text of the manuscript. All scientific content, critical analysis, and conclusions are entirely original, and no sections were autonomously generated by AI.

Acknowledgment: the authors thank the Duhok Medical Research Center for their support, technical assistance, and laboratory facilities during this investigation.